

components. This varies, of course, with the position ( $z$ ) along the "line of fire" as well as with the photon energy of the scattered radiation.

Figure 3 gives a picture of the results of this calculation. For purposes of comparison, the mean square radial displacement of the first scattered beam is also given (dashed lines).

At high energies the first scattered beam gets farther from the line  $\rho=0$  than the total scattered beam. This is because the photons of energy  $E$  which have been scattered two or more times have done much more of

their penetrating while they had an energy still greater than  $E$ . At these higher energies, the photons tended to stay close to the original "line of fire."

On the other hand, at low  $E$  and high  $z$  the total scattered beam tends to be farther from  $\rho=0$ . This is because the low energy photons do not travel far. If they appear very far from the original line they must have accomplished most of their radial displacement at an energy or energies greater than  $E$  but less than the source energy. This requires more than one scattering.

## Motion of a Ferromagnetic Domain Wall in $\text{Fe}_3\text{O}_4$

JOHN K. GALT

*Bell Telephone Laboratories, Murray Hill, New Jersey*

(Received October 25, 1951)

Experiments have been made on a sample of  $\text{Fe}_3\text{O}_4$  cut from a single crystal in such a way that its ferromagnetic domain pattern includes an individual domain wall whose motion can be studied. This sample has a permeability which is high (about 5000) at low frequencies and drops off rapidly above 1000 cycles. A hysteresis loop and data on wall velocity *vs* applied field were also taken. The data are discussed in terms of recent developments in the theory of the ferromagnetic domain wall. It appears that this theory explains our data satisfactorily, and that in using it to explain our data we determine some of the fundamental magnetic constants of  $\text{Fe}_3\text{O}_4$ . We are also able to gain some insight into domain wall motion in ferrites generally in this way.

### I. INTRODUCTION

LANDAU and Lifshitz<sup>1</sup> first discussed the relation between the velocity of a ferromagnetic domain wall and the field which causes it to move. They neglected eddy current effects. Williams and Shockley<sup>2</sup> have produced in silicon iron a domain boundary whose motion can be detected and studied. Eddy current effects are overwhelmingly important in determining the motion of a wall in this alloy, as they and Kittel<sup>3</sup> have shown, but these authors<sup>3</sup> have suggested that even in silicon iron the relaxation behavior of the spin system as discussed by Landau and Lifshitz may have an effect. The object of the present paper is to study the motion of a domain wall in  $\text{Fe}_3\text{O}_4$  where the eddy current effects are small enough so that the spin relaxation can be studied in a fairly direct manner. Our results will be shown to contain internal checks, and they will be compared with ferromagnetic resonance data. Furthermore it will be seen that our results are explainable in terms of recent theoretical developments and the Landau-Lifshitz results, and they therefore provide confirmation for these theories. It is therefore possible to produce a theory of the permeability of samples of certain shapes.

The sample used has a shape analogous to that of the rectangles used by Williams and Shockley,<sup>2</sup> being a polygonal ring with each leg along a direction of easy magnetization. Since the [111] direction is the direction of easy magnetization in  $\text{Fe}_3\text{O}_4$ , the ring was diamond-shaped with its face in the (110) plane, as shown schematically by the solid lines in Fig. 1. Each leg is 0.051 cm across and 0.102 cm thick as shown in Fig. 1.

The first samples studied were cut from natural crystals of  $\text{Fe}_3\text{O}_4$ , and they were unsuccessful. They required fields of the order of 30 oersteds to saturate, presumably because of such impediments to wall motion as cracks, imperfections, and impurities. It is in fact doubtful that they had the appropriate domain pattern at all. The successful final experiment was made possible by the growth of synthetic  $\text{Fe}_3\text{O}_4$  crystals<sup>4</sup> of high purity and mechanical perfection in the Laboratory for Insulation Research at the Massachusetts Institute of Technology. One such crystal was made available for these experiments by Professor von Hippel of that Laboratory.

### II. EXPERIMENTAL RESULTS

A hysteresis loop, data on wall velocity *vs* applied field, and data on permeability *vs* frequency were ob-

<sup>1</sup> L. Landau and E. Lifshitz, *Physik. Z. Sowjetunion* **8**, 153 (1935).

<sup>2</sup> H. J. Williams and W. Shockley, *Phys. Rev.* **75**, 178 (1949).

<sup>3</sup> Williams, Shockley, and Kittel, *Phys. Rev.* **80**, 1090 (1950).

<sup>4</sup> These crystals were grown under a contract sponsored jointly by the ONR, the Army Signal Corps, and the Air Force. See Progress Report V, Laboratory for Insulation Research, Massachusetts Institute of Technology, 1949, p. 58.

tained first, and observations were made on the domain pattern in the sample later. We will start the description of results with our observations of the domain pattern, however. The complete pattern has not been observed, as the sample was broken in the process of preparing it for these observations. Observations of the pattern on the sample, fitted back together after the break, however, show the essential features expected from the experience of Williams and Shockley.<sup>2</sup> This pattern, which consists of a movable wall all around the ring parallel to the (110) face of the sample and four stationary walls across the corners, is shown by the dotted lines in Fig. 1. A picture showing the intersection of the movable wall with the surface of the sample along one leg is shown in Fig. 2. The extra walls visible in Fig. 2 we attribute to the presence of the break in the sample. We have also observed some of the stationary walls across the corners of the sample. This picture was taken using the technique of Williams and Shockley.<sup>2</sup> The other data will be interpreted on the assumption that this pattern is correct, although the fracture of the sample has made it impossible to observe all its details.

In view of the incompleteness of the observations of the domain pattern, it seems desirable to comment on two alternative patterns which may seem plausible. First, if several parallel movable walls had been present, the hysteresis loop (see below) would have been somewhat different from that observed. Second, it may seem possible that the movable wall was in the  $(11\bar{2})$  plane, which is perpendicular to the (110) plane indicated above. This would produce a pattern more closely analogous geometrically to that observed by Williams and Shockley,<sup>2</sup> but aside from the fact that observations definitely indicate that this is not the pattern, the wall has twice the area and therefore approximately twice the energy if it is in the  $(11\bar{2})$  plane. The difference in our results which would be produced by changing the assumed pattern from one of these to another is not large and would not change any of our qualitative conclusions in any case.

Some experimentation with surface treatments was necessary before it was possible to observe the domain patterns of Fig. 2 on these artificially prepared surfaces. It was found quite easy to observe the pattern when the surface was clean and free down to the undisturbed material. The best procedure found for achieving this condition was to rub the ground surfaces of the original sample smooth with the finest emery cloth obtainable, and then to etch the sample by boiling it in 30 percent  $\text{H}_2\text{SO}_4$  for  $\frac{1}{2}$  to 1 hour under a reflux condenser.

The hysteresis loop of the sample, observed on the Cioffi recording fluxmeter,<sup>5</sup> is shown by the solid line in Fig. 3. It will be seen from Fig. 3 that the loop deviates from the square shape achieved in the silicon iron sample of Williams and Shockley.<sup>2</sup> It is felt that

<sup>5</sup> P. P. Cioffi, Phys. Rev. **67**, 200 (1945).

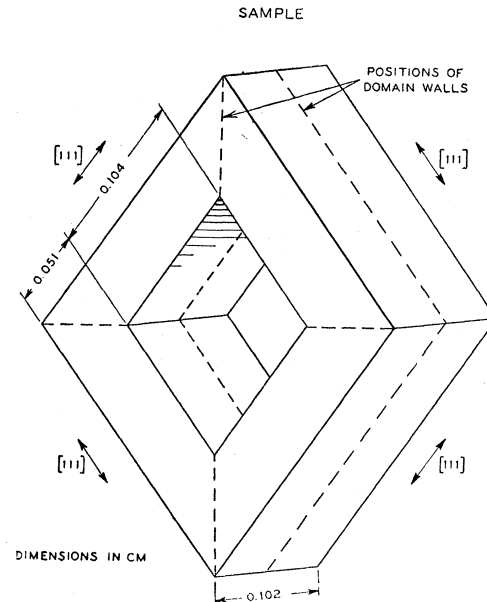


Fig. 1. Sample.

this is due to the fact that there were chips out of the sample so that the wall could not remain plane as it approached the sample faces, and a much larger field was therefore required to make it move in this region. By manipulating the field in the course of taking a loop such as that in Fig. 3, one finds that the actual loop has a bulge where the straight vertical portion begins and then contracts as shown by the dotted lines, so that the coercive force is actually only approximately 0.1 oersted. This effect has also been observed by Williams<sup>6</sup> in silicon iron rectangles. Maximum permeabilities read off the loop of Fig. 3 are approximately 25,000.



Fig. 2. Domain pattern on  $11\bar{2}$  plane which was outer face of a leg of the sample. The movable wall is indicated by white arrows. The other walls did not extend as far along the leg, and are therefore identified with the break in the sample. The edge of the sample runs from the top of the picture toward the left.

<sup>6</sup> Private communication.

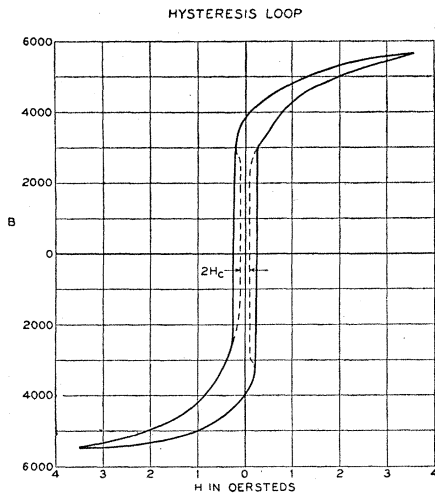


FIG. 3. Hysteresis loop.

Pulse techniques were used to obtain data on the relation between domain wall velocity and applied field. The sample was wound with a primary and a secondary winding, and the experiment was conducted as follows. A square pulse of positive voltage was applied to the primary winding in series with a resistor so that the rise time of this primary pulse was short compared to its length. This pulse was long enough so that the steady field it produced lasted for longer than the time required for the wall to move from one side of the sample to the other. The signal induced in the secondary winding was observed during this pulse on an oscilloscope whose sweep was synchronized with the pulser. A second pulse of negative voltage was applied to the primary during each duty cycle in order to bring the wall back to its original position. At low fields, a short high spike was introduced just at the start of the pulse in order to get the wall over the hump in the hysteresis loop shown by the dotted lines in Fig. 3. This initial spike had no effect on the subsequent motion.

The applied field due to the primary pulse  $H_{app}$  is deduced from the current in the primary winding and the solenoid formula  $H_{app} = 4\pi NI$ . To obtain the relation between wall velocity and induced voltage per secondary turn we have

$$\begin{aligned} \text{Volts/turn} &= (d\Phi/dt) \times 10^{-8} \\ &= 8\pi M_s (\Delta z/\Delta t) w_{wall} \times 10^{-8}, \quad (1) \end{aligned}$$

where  $\Delta z/\Delta t$  is equal to domain wall velocity  $v$ , and  $w_{wall}$  is the width of the wall between the boundaries of the sample in the direction perpendicular to the magnetization. The wall is at right angles to the direction of the velocity of course.

The calculation of wall velocity from the observed signal and Eq. (1) is of course based on the domain pattern. The results are shown in Fig. 4, where wall velocity is plotted *vs* applied magnetic field. It will be

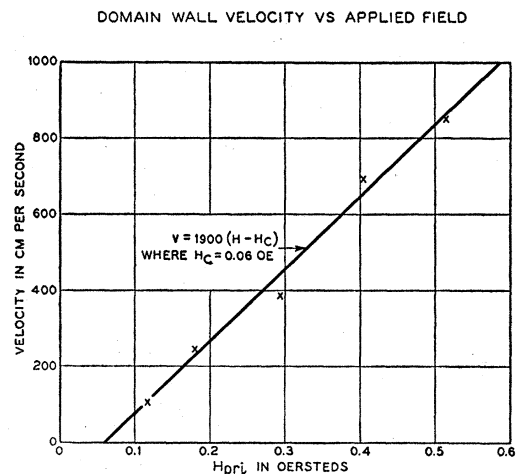
seen that we may write  $v = 1900(H_{app} - H_c)$  where  $H_c$  is approximately equal to the coercive force of 0.1 oersted as read from the hysteresis loop. It is clear that  $(H_{app} - H_c)$  is the field which is effective in producing wall motion. From the oscilloscope trace of wall velocity *vs* time it is clear that  $H_c$  varies as the wall moves, so that the value of  $H_c$  read from Fig. 4 is an average. The variations are essentially independent of applied field, however, as one would expect if they are caused in this way. Figure 5 is an example of one of the traces with the average velocity indicated by a straight line. One notices a fairly gradual decrease in velocity to zero, as one would expect from the hysteresis loop.

The data on initial permeability  $\mu (= \mu' - j\mu'')$  *vs* frequency at room temperature is given in Fig. 6. This data was obtained from bridge measurements<sup>7</sup> of the inductance of a coil wound on the sample. The data shows simple relaxation behavior as the frequency increases from low values where the wall follows the applied field to high values where it no longer can do so. The relaxation frequency is about 3000 cycles. The value of  $\mu'$  at low frequencies is comparable with the value read from the hysteresis loop at  $H=0$ , as we should expect. The instability of the wall, however, makes the value difficult to read from the hysteresis loop, so that this comparison cannot be made accurately.

The relaxation shown in Fig. 6 must be a domain wall relaxation since the permeabilities involved cannot be accounted for without invoking wall motion.

### III. THEORY

We will now correlate our data with recent theories of domain wall motion which start from the equation of motion of a unit area of the domain wall. We may use our data in this way to determine the constants of motion (mass, viscous resistance, and stiffness) of a

FIG. 4. Domain wall velocity *versus* applied field.

<sup>7</sup> W. D. Voelker, Bell Labs. Record **20**, 133 (1942).

unit area of wall. This point of view has been developed recently by Kittel,<sup>8</sup> Becker,<sup>9</sup> Rado,<sup>10</sup> and Döring.<sup>11</sup>

We consider unit area of a  $180^\circ$  domain wall between two regions of saturated magnetic material. Such a system has an equation of motion for small amplitudes of the applied magnetic field  $H$  which may be written

$$m\ddot{z} + \beta\dot{z} + \alpha z = 2M_s H, \quad (2)$$

where  $z$  is the displacement of the domain wall along its normal,  $m$  is its mass per unit area,  $\beta$  is a parameter measuring viscous resistance, and  $\alpha$  is a stiffness parameter measuring viscous resistance, and  $\alpha$  is a stiffness parameter, which has meaning only for small fields such as those used in initial permeability measurements. When fields larger than the coercive force are applied as in the experiment on wall velocity *vs* applied field, this term disappears and the effective field inside the material is less than the applied field by an amount equal to the coercive force; this is shown by Fig. 4. These results are quite reasonable when one remembers the spikes which pull back on the wall in the experiments of Williams and Shockley<sup>2</sup> for small wall motions and snap off entirely if the wall moves a large distance.

Let us consider the initial permeability data. We have for the relation between  $z$  and  $\mu$ ,

$$\mu = \Delta B / \Delta H = \Delta \Phi / A_{\text{coil}} \Delta H = 8\pi M_s z w_{\text{wall}} / A_{\text{coil}} H, \quad (3)$$

where  $w_{\text{wall}}$  is the width of the domain wall between the boundaries of the sample in a direction perpendicular to the magnetization and  $A_{\text{coil}}$  is the cross-sectional area of the coil around the sample. The general solutions of Eq. (2) for a sinusoidal applied field are too familiar to be reproduced here, but we note that Eq. (2) can be further simplified since we observe a relaxation mechanism (see Fig. 6). The values of  $\alpha$ ,  $\beta$ , and  $m$  will be calculated later; suffice it to say here that the order of magnitude of  $m$  is such that the first term on the left in Eq. (2) is negligible, and we may write

$$\beta\dot{z} + \alpha z = 2M_s H, \quad (4)$$

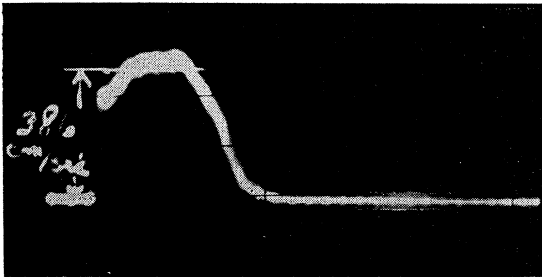


FIG. 5. Oscilloscope trace of secondary signal voltage *versus* time. The average velocity is shown by the horizontal straight line.

<sup>8</sup> C. Kittel, Phys. Rev. **79**, 214 (1950); Proceedings of Grenoble Conference (1950).

<sup>9</sup> R. Becker, Proceedings of Grenoble Conference (1950).

<sup>10</sup> Rado, Wright, and Emerson, Phys. Rev. **80**, 273 (1950).

<sup>11</sup> W. Döring, Z. Naturforsch. **3a**, 374 (1948).

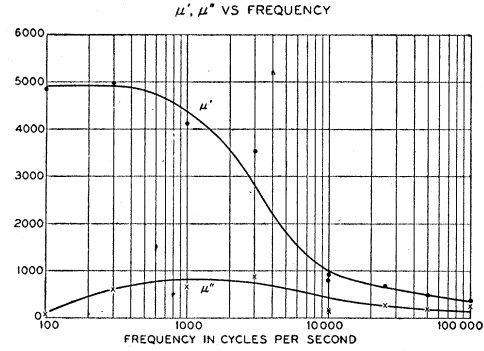


FIG. 6.  $\mu'$  and  $\mu''$  *versus* frequency.

which we may solve to give, if  $H = H_0 e^{i\omega t}$ ;

$$z = \frac{2M_s H_0}{\alpha} \left[ \frac{1}{1 + \omega^2 \beta^2 / \alpha^2} - \frac{j\omega \beta / \alpha}{1 + \omega^2 \beta^2 / \alpha^2} \right] e^{i\omega t}. \quad (5)$$

As the remarks above indicate, under the conditions of the experiment in wall velocity, Eq. (2) takes the form

$$\beta\dot{z} = 2M_s (H_{\text{app}} - H_c). \quad (6)$$

This relation obviously fits the data of Fig. 4.

We shall use Eqs. (5) and (6) later to derive values for  $\alpha$  and  $\beta$ .

We next carry the *theoretical* analysis one step further. The constants  $m$ ,  $\beta$ , and  $\alpha$  characterize a ferromagnetic domain wall. We now use the analysis originated by Landau and Lifshitz<sup>1</sup> for uniaxial crystals, and later developed by Kittel,<sup>12</sup> to derive  $\beta$  and  $m$  in terms of the constants which characterize the ferromagnetic material in general.

In order to derive  $\beta$  in this way, we calculate the power dissipated by a unit area of wall moving with velocity  $v$  in an applied field  $H_0$  from the equation of motion of the magnetization in a small volume. We then set this expression equal to  $2H_0 M_s v$  in order to find a relation between  $v$  and  $H_0$ , and  $\beta$  is derived by comparing this relation with (6). The equation of motion is

$$d\mathbf{M}/dt = \gamma[\mathbf{M} \times \mathbf{H}] - (\lambda/M^2)(\mathbf{M} \times [\mathbf{M} \times \mathbf{H}]). \quad (7)$$

The power dissipated per unit volume is  $\mathbf{H} \cdot d\mathbf{M}/dt$ , which is

$$\mathbf{H} \cdot d\mathbf{M}/dt \cong \lambda H_e^2, \quad (8)$$

where  $\mathbf{H} = \mathbf{H}_0 + \mathbf{H}_e$ ,  $\mathbf{H}_0$  is the applied field and  $\mathbf{H}_e$  is a field associated with the motion of the wall as Becker<sup>9</sup> has shown. It exists only in the wall and is perpendicular to the wall. The value of this field is determined from the precessional angular velocity of the spins in the moving wall by means of the Larmor relation. It is

$$\mathbf{H}_e = -(\mathbf{v}/\gamma)(\partial\theta/\partial z), \quad (9)$$

where  $\gamma$  is the gyromagnetic ratio and  $\theta$  is the rotational

<sup>12</sup> C. Kittel, Phys. Rev. **80**, 918 (1950).

angle of the spins in a  $180^\circ$  wall. In the theory of the domain wall<sup>13</sup> it is shown that

$$\partial\theta/\partial z = [g(\theta)/A]^{\frac{1}{2}}, \quad (10)$$

where  $A$  is a measure of the exchange energy per unit volume due to gradients in the direction of the magnetization as given by Eq. (11).

$$\text{Exchange energy/unit vol.} = A[(\nabla\alpha_1)^2 + (\nabla\alpha_2)^2 + (\nabla\alpha_3)^2]. \quad (11)$$

Here  $\alpha_1, \alpha_2, \alpha_3$  are the direction cosines of the magnetization.  $g(\theta)$  is the anisotropy energy density

$$g(\theta) = K_1(\alpha_1^2\alpha_2^2 + \alpha_2^2\alpha_3^2 + \alpha_3^2\alpha_1^2), \quad (12)$$

expressed in terms of  $\theta$ .  $K_1$  is the first-order anisotropy constant.

If we use Eqs. (9) and (10) in Eq. (8) and integrate over  $z$  to get the power dissipated for unit area of wall, we have

$$\int_{-\infty}^{\infty} \mathbf{H} \cdot \frac{d\mathbf{M}}{dt} dz = 2H_0 M_s v = (\lambda v^2 / \gamma^2 A^{\frac{1}{2}}) \int_0^\pi [g(\theta)]^{\frac{1}{2}} d\theta, \quad (13)$$

where we have used Eq. (10) to transform from integration over  $z$  to integration over  $\theta$  as well as to evaluate Eq. (9). We may now write

$$v = \frac{2M_s \gamma^2 A^{\frac{1}{2}}}{\lambda \int_0^\pi [g(\theta)]^{\frac{1}{2}} d\theta} H_0. \quad (14)$$

This is the desired relation between  $v$  and  $H_0$  which is to be compared with Eq. (6). In this way we find

$$\beta = (\lambda / \gamma^2 A^{\frac{1}{2}}) \int_0^\pi [g(\theta)]^{\frac{1}{2}} d\theta. \quad (15)$$

We derive  $m$  from the energy of motion of the wall, which we equate to  $\frac{1}{2}mv^2$ . This was first done by Becker.<sup>9</sup> He pointed out that this energy was equal to  $(1/8\pi) \int H_e^2 dV$ , and by means of Eq. (9) he was able to write

$$m = (1/4\pi\gamma^2) \int_{-\infty}^{\infty} \left( \frac{\partial\theta}{\partial z} \right)^2 dz. \quad (16)$$

If we use Eqs. (10), (11), and (12) this becomes

$$m = (1/4\pi\gamma^2 A^{\frac{1}{2}}) \int_0^\pi [g(\theta)]^{\frac{1}{2}} d\theta. \quad (17)$$

It will be noted that the above analyses neglect the effect of eddy currents. As Williams, Shockley, and Kittel<sup>3</sup> have shown, these will contribute part of the measured value of the ratio of  $v$  to  $H_0$  and of the damping constant  $\beta$  which also affects the data of

<sup>13</sup> C. Kittel, *Revs. Modern Phys.* **21**, 541 (1950); see Eq. (3.3.9).

Fig. 6. The equations of Williams, Shockley, and Kittel will be used in the next section to correct the data for eddy current effects.

#### IV. DISCUSSION

If we evaluate the various factors in Eq. (15), we can use it to evaluate  $\lambda$  from the data given in Fig. 4. Since the wall is in a (110) plane, we have

$$g(\theta) = \frac{1}{4}K_1[\cos^4(\theta + 35^\circ 16') + \sin^2 2(\theta + 35^\circ 16')], \quad (18)$$

where  $\theta=0$  on one side of the wall and  $\pi$  on the other. Then,

$$\int_0^\pi [g(\theta)]^{\frac{1}{2}} d\theta = 1.38 |K_1|^{\frac{1}{2}}. \quad (19)$$

In performing this integration, care must be taken to use the positive value of the square root over the whole interval. The evaluation of  $A$  requires some discussion. It may be done from the Curie constant and the Curie temperature as described by Néel.<sup>14</sup> This method gives  $A = 5.62 \times 10^{-7}$  if we use the data of Kopp<sup>15</sup> to evaluate the Curie constant. This evaluation of the Curie constant is unsatisfactory, however, since (as Néel<sup>16</sup> has later shown it should) the reciprocal of the susceptibility above the Curie temperature follows a curved line. A more satisfactory evaluation can be made from a fundamental relation recently derived by Herring and Kittel<sup>17</sup> between  $A$  and the Bloch constant:

$$A = [S_0/\Omega]^{\frac{1}{2}} [k/13.3C^{\frac{1}{2}}], \quad (20)$$

where  $k$  is Boltzmann's constant,  $C$  is Bloch's constant as used in the relation  $M_s = M_0(1 - CT^{\frac{1}{2}})$ ,  $S_0$  is the atomic spin, and  $\Omega$  is the atomic volume. ( $S_0/\Omega$ ) is equal to the saturation magnetization at  $0^\circ\text{K}$  divided by the Bohr magneton. From (20) we find  $A = 1.53 \times 10^{-6}$ , and this is the value we shall use. The Bloch constant used in this evaluation ( $C = 4 \times 10^{-6}$ ) was obtained by fitting the Bloch  $T^{\frac{1}{2}}$  law to the saturation magnetization measurements of Weiss and Forrer.<sup>18</sup> Because of the square root in (13), the value of  $\lambda$  we obtain will not depend critically on the value used for  $A$ . Using  $M_s = 460$  cgs units at room temperature,  $\gamma = 1.76 \times 10^7$  and  $K_1 = -1.1 \times 10^6$  ergs/cc as given by Bickford,<sup>19</sup> we find for  $\text{Fe}_3\text{O}_4$  from Eq. (14),

$$v/H_0 = 7.7 \times 10^{11}/\lambda. \quad (21)$$

The data in Fig. 4 give  $v/H_0 = 1900$ . Before using this in (21) to calculate  $\lambda$ , however, we must correct for eddy current losses. Equation (6) may be written in the form

$$\beta \dot{z} = (\beta_e + \beta_r) \dot{z} = 2M_s(H_{\text{app}} - H_c), \quad (22)$$

<sup>14</sup> L. Néel, *Cahiers Physique* **25a**, 1 (1944).

<sup>15</sup> W. Kopp, thesis, Zurich (1919).

<sup>16</sup> L. Néel, *Ann. phys.* **3**, 137 (1948).

<sup>17</sup> C. Herring and C. Kittel, *Phys. Rev.* **81**, 869 (1951); see Eq. (5).

<sup>18</sup> P. Weiss and R. Forrer, *Ann. phys.*, series 10, **12**, 279 (1929).

<sup>19</sup> L. R. Bickford, Jr., *Phys. Rev.* **78**, 449 (1950).

where  $\beta_e$  measures the contribution due to eddy currents and  $\beta_r$  measures the effect described by Eq. (21). From Fig. 4 we now have  $\beta_e + \beta_r = 2M_s/1900 = 0.484$ . From the low field approximation for eddy current effects given by Williams, Shockley, and Kittel (see reference 3, Eq. (11)) we find  $\beta_e = 0.078$ . Hence, experimentally,

$$\beta = 0.484, \quad \beta_r = 0.406, \quad (23)$$

for  $\text{Fe}_3\text{O}_4$ . From Eqs. (21) and (22)  $7.7 \times 10^{11}/\lambda = 2M_s/\beta_r$ , and we find

$$\lambda = 3.5 \times 10^9. \quad (24)$$

It is appropriate to compare this with the value determined from the ferromagnetic resonance line width observed by Bickford.<sup>19</sup> His line width at half-power points for magnetic absorption is approximately 1500 oersted. The relation between line width and  $\lambda$  has been given elsewhere.<sup>20</sup> Sample shape enters into this relation, but not in a critical way, and we therefore ignore it except as it affects  $H_{\text{res}}$ . The relation is

$$2\Delta H \gamma M_s / H_{\text{res}} = \lambda, \quad (25)$$

where the line width is  $2\Delta H$ . From Bickford's data and Eq. (25) we find  $\lambda = 1.9 \times 10^9$ . Thus our value predicts a line about  $\frac{1}{2}$  as wide as Bickford's.

The difference between our value for  $\lambda$  and Bickford's may be due at least partly to field inhomogeneities in the samples used by Bickford. Such inhomogeneities have been observed to affect ferromagnetic resonance line widths in ferrite samples,<sup>20,21</sup> and Bickford's samples were large enough to indicate that such effects are expected.

All the factors in Eq. (17) have now been evaluated, and when we make the numerical calculation we find  $m = 9.5 \times 10^{-11}$  g/cm<sup>2</sup>. This value is so small that the first term in Eq. (2) does not affect our experiments significantly.

From  $\beta = \beta_e + \beta_r$  as given by Eq. (23), and from Fig. 6 using Eqs. (3) and (5) we can determine  $\alpha$  for our sample. We note that  $\mu'$  has dropped to  $\frac{1}{2}$  its value at low frequency when  $\omega\beta/\alpha = 1$ . Figure 6 shows that this occurs at 3000 cycles. In this way we find

$$\alpha = 9100. \quad (26)$$

<sup>20</sup> Yager, Galt, Merritt, and Wood, Phys. Rev. **80**, 744 (1950); see Eq. (A-6). The  $\lambda$  of the present paper is equal to  $\gamma\alpha M_s$  in the notation of this reference.

<sup>21</sup> Yager, Merritt, and Guillaud, Phys. Rev. **81**, 477 (1950).

We can also check our value of  $\beta$  by determining it from the data of Fig. 6. If we make a reasonable estimate of  $A_{\text{coil}}$  from the cross-sectional area of a leg of the sample and the thickness of the windings, we may use Eqs. (3) and (5) to find  $\alpha$ . We may then derive  $\beta$  from the fact that  $\omega\beta/\alpha = 1$  at  $\omega = 2\pi \times 3000$ . This leads to  $\beta = 0.5$ , which checks the value given in Eq. (23) satisfactorily. The accuracy of the check is not as good as we should like, however, as it was impossible actually to measure  $A_{\text{coil}}$ . It is hoped that this can be done when larger samples are available for these experiments.

It should be emphasized that  $\beta$  is a fundamental property of the material whereas  $\alpha$  is a constant characteristic only of a particular sample. As Eq. (2) shows,  $\alpha$  measures the rate at which magnetostatic energy is built up as the position of the wall changes, and in our sample it has a uniquely low value. If it were increased, as it would be if the sample shape were such that the wall could not move so easily without building up a magnetic field, the permeability at low frequency would drop, the relaxation frequency for  $\mu$  would increase, and the wall motion might begin to show resonant behavior. Bickford<sup>19</sup> has given a permeability for  $\text{Fe}_3\text{O}_4$  at room temperature of about 45 in a sample where the domain pattern is not controlled, but in which we may think of the effective  $\alpha$  as being enough higher than ours to reduce  $\mu'$  from our value (4900) to his.

It may be noted here that single crystal samples of the shape and orientation used in these experiments may be of use in devices involving saturable reactors such as memory devices and magnetic amplifiers.

## V. ACKNOWLEDGMENTS

The author wishes to express his gratitude to several friends and colleagues for assistance with various aspects of this research. The crystal from which the sample was cut was provided by Professor von Hippel of the Laboratory for Insulation Research at MIT.<sup>4</sup> H. J. Williams has been of considerable help in observing the domain patterns. W. L. Bond and J. Andrus cut the samples from bulk crystal. The author has had useful conversations with C. Kittel, R. M. Bozorth, C. L. Luke, and W. Yocum. H. G. Hopper has given technical assistance with all the work, and technical assistance on specific points was given by P. P. Cioffi, C. D. Owens and R. G. Conway, R. D. Heidenreich, H. R. Moore, and N. R. Pape.



FIG. 2. Domain pattern on  $11\bar{2}$  plane which was outer face of a leg of the sample. The movable wall is indicated by white arrows. The other walls did not extend as far along the leg, and are therefore identified with the break in the sample. The edge of the sample runs from the top of the picture toward the left.

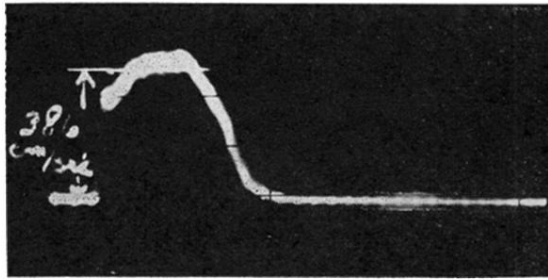


FIG. 5. Oscilloscope trace of secondary signal voltage *versus* time. The average velocity is shown by the horizontal straight line.